Probing the phosphoinositide 4,5-*bis*phosphate binding site of human profilin I

Anu Chaudhary[1,2*], Jian Chen[1,2], Qu-Ming Gu[2], Walter Witke[3†], David J Kwiatkowski[3] and Glenn D Prestwich[1,2]

Background: Profilin is a widely and highly expressed 14 kDa protein that binds actin monomers, poly(L-proline) and polyphosphoinositol lipids. It participates in regulating actin-filament dynamics that are essential for many types of cell motility. We sought to investigate the site of interaction of profilin with phosphoinositides.

Results: Human profilin I was covalently modified using three tritium-labeled 4-benzoyldihydrocinnamoyl (BZDC)-containing photoaffinity analogs of phosphatidylinositol 4,5-*bis*phosphate (PtdIns(4,5)P_2). The P-1-tethered D-*myo*-inositol 1,4,5-*tris*phosphate (Ins(1,4,5)P_3) modified profilin I efficiently and specifically; the covalent labeling could be displaced by co-incubation with an excess of PtdIns(4,5)P_2 but not with Ins(1,4,5)P_3. The acyl-modified PtdIns(4,5)P_2 analog showed little protein labeling even at very low concentrations, whereas the head-group-modified PtdIns(4,5)P_2 phosphotriester-labeled monomeric and oligomeric profilin. Mass spectroscopic analyses of CNBr digests of [^{3}H]BZDC–Ins(1,4,5)P_3-modified recombinant profilin suggested that modification was in the amino-terminal helical CNBr fragment. Edman degradation confirmed Ala1 of profilin I (residue 4 of the recombinant protein) was modified. Molecular models show a minimum energy conformation in which the hydrophobic region of the ligand contacts the amino-terminal helix whereas the 4,5-*bis*phosphate interacts with Arg135 and Arg136 of the carboxy-terminal helix.

Conclusions: The PtdIns(4,5)P_2-binding site of profilin I includes a *bis*phosphate interaction with a base-rich motif in the carboxy-terminal helix and contact between the lipid moiety of PtdIns(4,5)P_2 and a hydrophobic region of the amino-terminal helix of profilin. This is the first direct evidence for a site of interaction of the lipid moiety of a phosphoinositide *bis*phosphate analog with profilin.

Addresses: [1]Departments of Chemistry, Biochemistry and Cell Biology, The University at Stony Brook, Stony Brook, New York 11794-3400, USA. [2]The University of Utah, Department of Medicinal Chemistry, 30 South, 2000 East, Room 201, Salt Lake City, Utah 84112-5820, USA. [3]Division of Hematology–Oncology, and Experimental Medicine, Department of Medicine, Brigham and Women's Hospital, Harvard Medical School, Boston, Massachusetts 02115, USA.

Present addresses: *Harvard Medical School, Department of Cell Biology, 240 Longwood Avenue, Boston, Massachusetts 02115, USA. †EMBL, Meyerhoffstrasse 1, Postfach 10.6629, 69012 Heidelberg, Germany.

Correspondence: Glenn D Prestwich (in Utah)
E-mail: gprestwich@deans.pharm.utah.edu

Key words: actin-binding protein, MALDI–TOF, phosphatidylinositol, photoaffinity, profilin

Received: **6 October 1997**
Revisions requested: **4 November 1997**
Revisions received: **18 March 1998**
Accepted: **15 April 1998**

Published: **8 May 1998**

Chemistry & Biology May 1998, **5**:273–281
http://biomednet.com/elecref/1074552100500273

Introduction

Profilins are abundant small proteins (12–15 kDa), found in all eukaryotic cells, that bind to actin, proline-rich sequences and phosphatidylinositol 4,5-*bis*phosphate (PtdIns(4,5)P_2) *in vitro*. They have been proposed to function as cellular regulators that link transmembrane signal transduction to the reorganization of the actin cytoskeleton required for cell motility [1,2]. Hydrolysis of PtdIns(4,5)P_2 by phospholipase C-γ (PLC-γ) leads to the production of the second messengers inositol *tris*phosphate (Ins(1,4,5)P_3) and diacylglycerol. The activity of PLC-γ on PtdIns(4,5)P_2 is inhibited by the binding of profilin to PtdIns(4,5)P_2, an event associated with the activation of receptor tyrosine kinases [3,4]. PtdIns(4,5)P_2 metabolism has, in turn, been implicated in the localization of profilin. Profilin binds dynamically to cell membranes *in vivo* [5], and depletion of PtdIns(4,5)P_2 in response to external signals appears to mediate the translocation of profilin from the plasma membrane to the cytosolic fraction [6]. Profilin and gelsolin also increase phosphoinositide (PI) 3-kinase activity [7]. Profilin binds poly-(L-proline) [8,9] with high affinity, and this property appears to reflect the binding of profilin to the vasodilator-associated phosphoprotein *in vivo* [10]. The multiple binding properties of profilin are intriguing and many interpretations of the physiological significance of a particular binding affinity have been suggested.

Humans express two isoforms of profilin, I and II, that differ in their pI (8.4 and 5.9, respectively) and in their affinity for monomeric actin, but they have similar affinities for PtdIns(4,5)P_2 and poly-(L-proline) [11–13]. From lower eukaryotes to humans, the primary structures of profilin I and II have diverged significantly among species and between the isoforms. Approximately 25% of the amino acids are identical between human profilin I and either *Acanthamoeba* or *Dictyostelium* profilin I. Plant profilins have been reported to be conserved with other classes of profilins [14]. Further evidence for the critical importance of profilin function *in vivo* is provided by the observation that *Dictyostelium* mutants lacking both forms of profilin have

marked deficiencies in cytokinesis and development [15]. In addition to the evolutionary conservation of profilin, studies in several organisms have implicated profilin as an important protein in many aspects of cell function [15–19]. On the basis of analyses in the lower eukaryotic organisms, profilin appears to be critically important in cytokinesis. Studies of the motile processes (ruffles, filopodia) in fibroblasts and other vertebrate cell types, however, indicate that profilin probably participates with actin-filament-bared end-binding proteins and actin-related proteins to control the site and extent of actin-filament assembly during motility [20–22]. Finally, despite the presence of two isoforms of profilin in humans, deletion of profilin I is lethal in mice at a very early stage, prior to blastocyst development [23].

The poly-(L-proline)-binding site of profilins has been reported to be the most highly conserved feature [9,14]. The actin-binding surface on the protein is not conserved [14,24]. The location of the PtdIns(4,5)P_2-binding sites on profilins are debated, and conflicting data have been generated by several laboratories. In some cases, differences could arise from the use of synthetic dipalmitoyl-PtdIns(4,5)P_2, as opposed to the naturally occurring *sn*-1-*O*-stearoyl-2-*O*-arachidonyl PtdIns(4,5)P_2, leading to different protein–ligand interactions. Basic residues are predicted to be essential for binding of the phosphate head groups. Evidence has been presented implicating the carboxy-terminal region in which four positive residues reside in human profilin I (profilin I (126–136)) [25], and a central region containing several additional dispersed basic residues (profilin I (69–125)) [26]. In addition, the intrinsic fluorescence of Trp3 and Trp31 is quenched by PtdIns(4,5)P_2 binding [27]. Arg88 has also been demonstrated to be essential for PtdIns(4,5)P_2 binding by human profilin I; a decapeptide containing arginine is capable of binding PtdIns(4,5)P_2 with relatively high affinity [28]. PtdIns(4,5)P_2 has also been shown to compete for binding of profilin I to poly-(L-proline) [13]. In addition, the D-3 phosphoinositides have shown high affinity for human profilin, with dipalmitoyl-PtdIns(3,4)P_2 having a tenfold greater affinity than dipalmitoyl-PtdIns(4,5)P_2 [29]. The PtdInsP_2-binding sites on human profilin may also include an exposed hydrophobic cluster located between the amino-terminal and the carboxy-terminal helices, in conjunction with the central barrel of β sheets [24].

To explore the interactions of the diacylglyceryl sidechains of PtdIns(4,5)P_2 with human profilin I, we examined the binding specificity and affinity of three photoactivatable analogs of PtdIns(4,5)P_2 [30–32]. We then employed one of these probes to identify amino acids of recombinant human profilin I in contact with the hydrophobic region of PtdIns(4,5)P_2. The three tritium-labeled PtdIns(4,5)P_2 photoaffinity analogs used for these studies were selected in order to sample different spatial regions, including both the lipid bilayer environment and the head group (bilayer/water) interface [33].

Results

Three photoaffinity probes (Figure 1) that are structurally analogous to PtdIns(4,5)P_2 were used to probe the selectivity and specificity of the profilin I–PtdIns(4,5)P_2 interactions. Each of these photoaffinity labels [30–32] had the same nominal specific activity, 35–42.5 Ci/mmol, as determined by the specific activity of the batch of [^{3}H]4-benzoyldihydrocinnamoyl–*N*-hydroxysuccinimide (BZDC–NHS) ester employed.

To determine the selectivity of the PtdIns(4,5)P_2 photoanalogs for human profilin I, photoaffinity-labeling studies were performed using three probes, [^{3}H]BZDC–Ins(1,4,5)P_3, [^{3}H]BZDC–*acyl*-PtdIns(4,5)P_2 and [^{3}H]BZDC–*triester*-PtdIns(4,5)P_2 (see Figure 2). The specificity of these probes was determined by studying competition with 1,000-fold excess of Ins(1,4,5)P_3, PtdIns(4,5)P_2 or adenophostin A (an Ins(1,4,5)P_3 receptor hyperagonist [34,35]). Both PtdIns(4,5)P_2 and adenophostin A displaced the labeling by [^{3}H]BZDC–Ins(1,4,5)P_3 (Figure 2a), but the soluble head group, Ins(1,4,5)P_3, failed to displace the photoinduced covalent labeling. Adenophostin A apparently has both the necessary *bis*phosphate recognition element in conjunction with a hydrophobic tail that, as with the photophoric group of [^{3}H]BZDC–Ins(1,4,5)P_3, mimics the lipid moiety of the PtdIns(4,5)P_2 diacylglyceryl moiety. Only adenophostin A displaced labeling by [^{3}H]BZDC–*triester*-PtdIns(4,5)P_2 (Figure 2b), and it appears that the ligand PtdIns(4,5)P_2 increased labeling by this probe. In Figure 2c, the labeling of profilin I with the [^{3}H]BZDC–*acyl*-PtdIns(4,5)P_2 probe shows modest labeling of a 14 kDa band; the heavily labeled band at the dye front suggests that the micellar photoprobe may give rise to photo-cross-linked phospholipid micelles, as the labeled band shows no staining with Coomassie Blue. Interestingly, incorporation of 1 mM Ca^{2+} in the photoaffinity-labeling buffer inhibited labeling of all [^{3}H]BZDC probes (data shown for [^{3}H]BZDC–Ins(1,4,5)P_3 in Figure 2d) but reversed the effects of PtdIns(4,5)P_2 displacement or enhancement (see lane 5 in Figure 2a,b).

The effects of divalent metal ions on profilin labeling were examined by incorporation of metal salts in the photolabeling buffer. The [^{3}H]BZDC–Ins(1,4,5)P_3 labeling showed an interesting metal-ion dependence (see Figure 2d). In the presence of 1 mM Ca^{2+}, no labeling of the protein was observed. Addition of 1 mM Ba^{2+} ions led to band broadening and dramatically enhanced labeling of profilin monomers and higher oligomers. Incorporation of Mg^{2+}, K^+ or EGTA had no effect on the labeling, whereas the addition of Sr^{2+} resulted in a definite enhancement of monomer and dimer labeling.

To determine the hydrophobic region of profilin involved in diacylglycerol binding, [^{3}H]BZDC–Ins(1,4,5)P_3 was thus selected as the photoprobe of choice. This photolabel

Figure 1

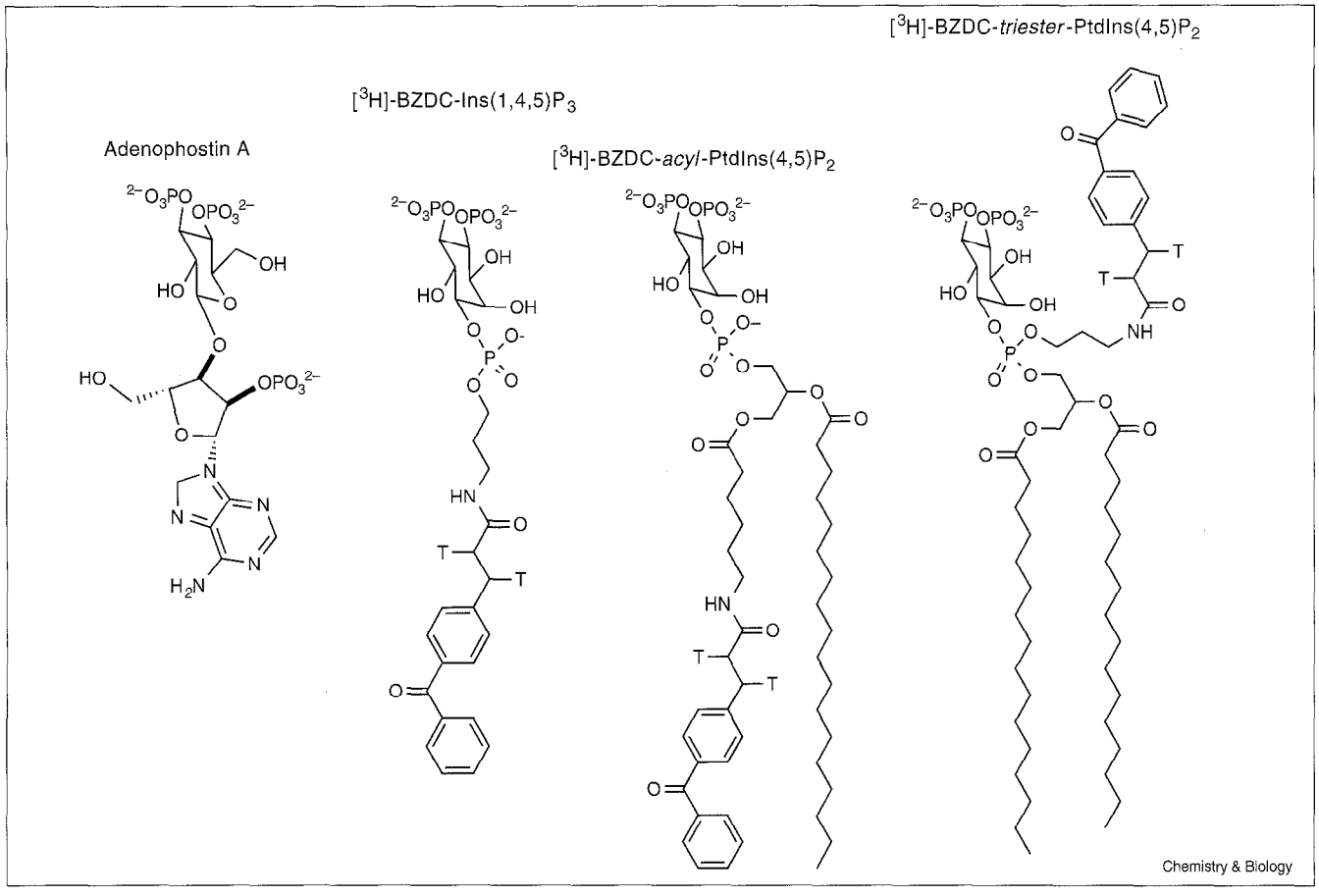

Structures of adenophostin A and three PtdIns(4,5)P_2 photoaffinity analogs (T = ^{1}H or ^{3}H) shown in polybasic forms.

showed highly specific labeling that was not displaced by the soluble head group alone but was displaced by dipalmitoyl PtdIns(4,5)P_2. Moreover, unlike the polyphosphoinositides and their analogs, BZDC–Ins(1,4,5)P_3 showed no propensity for micelle formation at the concentrations used. Trichloroacetic acid precipitation and an acetone wash removed unreacted probe following the photocovalent labeling. Importantly, this probe and related analogs have been successfully used to identify the binding site of the cerebellar Ins(1,4,5)P_3 receptor [36] as well as the pleckstrin homology (PH) domain of the δ_1 isoform of PLC [37,38].

Six fragments were predicted for the CNBr digestion of profilin I, taking into account the three amino-terminal amino acids (Gly–Ser–Met; GSM) generated from the bacterial expression of profilin I [11]. CNBr digestion was performed according to standard protocols [39].

First, the crude CNBr digests of unmodified and photoaffinity-modified profilin I were analyzed by matrix-assisted laser desorption/ionization-time-of-flight (MALDI–TOF) mass spectroscopy (MS) to a resolution of ± 0.12%. The mass spectra of the CNBr digests of the unlabeled profilin I and the BZDC–Ins(1,4,5)P_3-labeled samples were compared. In the unlabeled profilin, fragment 2 (amino acids 4–14, AGWNAYI; calc'd, 1218.5, found, 1217.8) was the most prominent feature. In the digest of BZDC–Ins(1,4,5)P_3-labeled profilin I, the peak for fragment 1 was diminished and a prominent new peak at m/z 1506.8, not present in the unlabeled digest, was observed. This could be assigned to fragments 1 + 2 (amino acids 1–14, GSMAGWNAYI) with an additional oxygen (calc'd, 1509.6). Such a fragment would correspond to the presence of an uncleaved Met–Ala bond, possibly resulting from photoinduced S-oxidation of the internal methionine residue. The evidence for lack of cleavage of Met3–Ala4 in the labeled compared with the unlabeled profilin was reproducible in several independent trials. We were unable to directly observe a fragment attributable to a BZDC–Ins(1,4,5)P_3-containing fragment, however.

Thus, a second approach was taken. The CNBr digest of modified profilin I was separated by reverse-phase high

Figure 2

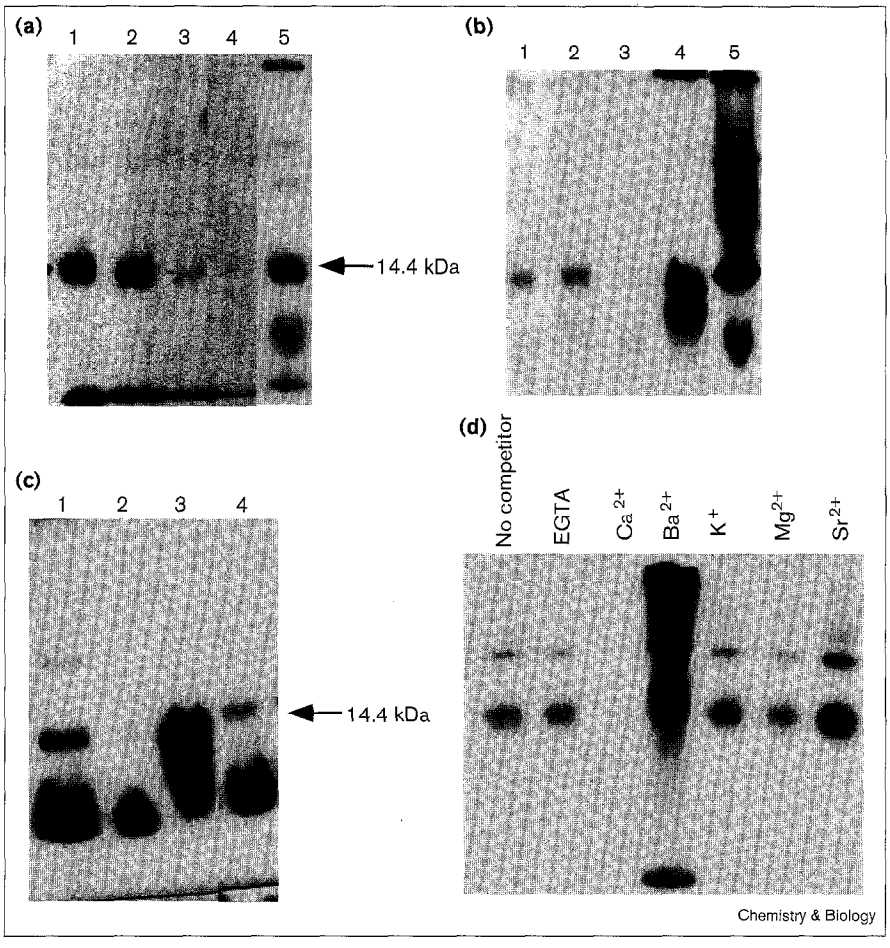

Photoaffinity labeling of human profilin I with the three [^{3}H]BZDC probes (Ins(1,4,5)P_3; *triester*-PtdIns(4,5)P_2 and *acyl*-PtdIns(4,5)P_2). Fluorograms of the SDS–18% PAGE are shown. For **(a–c)**, the protein was labeled (45 min, 4°C, 360 nm) with 0.4 μCi (0.1 μM) of the [^{3}H]BZDC probe in buffer A (see text), in the absence (lane 1) or presence of a 1,000-fold excess of Ins(1,4,5)P_3 (lane 2), adenophostin A (lane 3) or PtdIns(4,5)P_2 (lane 4) as competing ligands. Lane 5 is lane 4 with 1 mM Ca^{2+} in the buffer. (a) Data for [^{3}H]BZDC–Ins(1,4,5)P_3 as photoaffinity label; (b) data for [^{3}H]BZDC–*triester*-PtdIns(4,5)P_2 probe; (c) data for [^{3}H]BZDC–*acyl*-PtdIns(4,5)P_2 probe. **(d)** The effect of metal ions on photoaffinity labeling of human profilin I with [^{3}H]BZDC–Ins(1,4,5)P_3. Metal ions (1 mM) were added to the incubation as described for (a).

performance liquid chromatography (HPLC) to obtain peptide fragments that retained the radioactive label of the attached [^{3}H]BZDC–Ins(1,4,5)P_3. Two major radioactive fractions were eluted from the C_{18} column, but only one of these (containing 0.05% of the total radioactivity) could be sequenced by Edman degradation. This sequence, GSMAGWNAYI, corresponded to the amino-terminal amino acid residues of the cleaved recombinant protein, but, surprisingly, contained an internal methionine residue that would have been expected to undergo cleavage in the presence of CNBr. Liquid scintillation counting (LSC) of the radioactivity in each amino acid phenylthiohydantoin derivative fraction indicated that Ala4 (Ala1, native protein numbering) was photocovalently labeled (Figure 3). The covalent labeling of alanine probably occurs via H abstraction of the C_α methine or C_β methylene [40,41]. The covalent modification of the alanine residue may also locate the carbonyl oxygen of the benzophenone in a suitable position to allow methionine oxidation as an alternative pathway, leading to the MALDI–TOF MS data described above.

An energy-minimized model of profilin I with BZDC–Ins(1,4,5)P_3 was calculated using the average solution structure of human profilin I [3]. This structure was then equilibrated with the ligand, after the carbonyl oxygen of the benzophenone was fixed at a distance of 3.0 Å from the C_α-H on Ala4 (Ala1 of native profilin I). Figure 4 shows the calculated complex between profilin I and BZDC–Ins(1,4,5)P_3. The constraint imposed on the location of the carbonyl oxygen adjacent to Ala1 of the amino-terminal helix permits a minimum energy conformation that allows interaction of the 4,5-*bis*phosphate moiety with Arg135 and Arg136 of the carboxy-terminal helix.

Discussion

Photoactivatable analogs of inositol polyphosphates ($InsP_n$s) and phosphoinositide polyphosphates ($PtdInsP_n$s) [33] have enabled identification of a large number of $InsP_n$- or $PtdInsP_n$-binding proteins [41]. These tethered ligands have proven to be extremely site selective and protein selective, and were designed such that linkage to the photophore should not substantially interfere with important binding interactions between the protein and the phosphoinositide phosphates. Benzophenone probes have found extensive application as photoprobes for studying $InsP_n$- and $PtdInsP_n$-binding proteins significant in cell signaling and

Figure 3

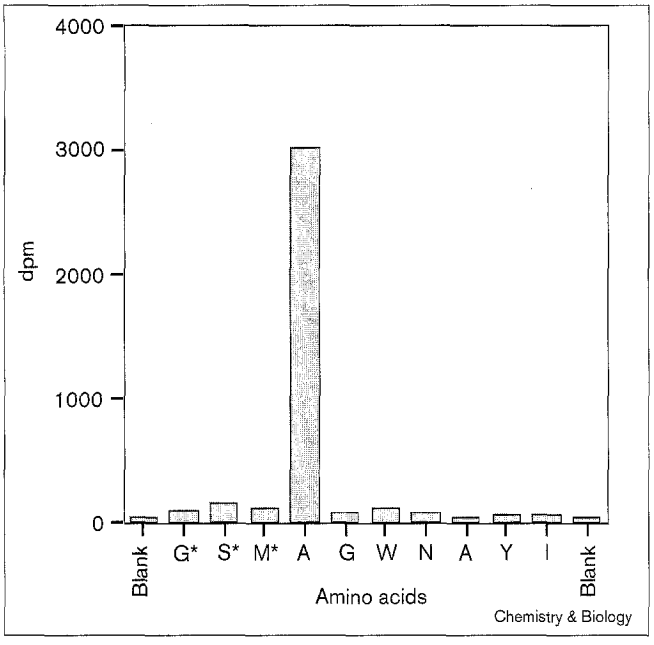

Radiosequencing of the CNBr-digested radiolabeled peptide. The radiolabeled fragment was obtained by HPLC and sequenced by Edman degradation. *Amino acids remaining following bacterial processing from pMW172 vector construct. The single-letter amino-acid code is used.

Figure 4

Two energy-minimized representations of the interaction of human profilin I with BZDC–Ins(1,4,5)P_3. Coordinates from the Brookhaven Database were downloaded, an energy-minimized structure for BZDC–Ins(1,4,5)P_3 was obtained separately, and the two structures were docked by fixing the carbonyl oxygen of the benzophenone at a distance of 3.0 Å from the Ala1 C_α–H. **(a)** A van der Waals depiction of the protein (grey) and a stick model of the ligand. Ala1 C_α–H (light blue), proximal to the benzophenone carbonyl (green/red); the 4,5-*bis*phosphate residues (purple) interact with Arg135 and Arg136 protonated guanidinium nitrogens (dark blue) in this model. **(b)** A close-up ribbon model of the docking of the BZDC–Ins(1,4,5)P_3 (color) between the carboxy-terminal (center) and amino-terminal (left) helices of profilin I.

protein trafficking [41]. Typically, the benzophenone photophore in biochemical systems is most regioselective when the tether is limited to a four to eight atom linker that permits flexibility for an efficient H-abstraction (for detailed reviews see [40,41]). Thus, $InsP_n$ and $PtdInsP_n$ analogs that have *O*-aminopropyl-linked BZDC (or related) photophores [33,41] have proven useful in active-site modification of Ins(1,4,5)P_3 [36], Ins(1,3,4,5)P_4 [42,43], $InsP_6$ [42], PtdIns(4,5)P_2 [38] and PtdIns(3,4,5)P_3 [44] binding proteins. The [^{3}H]BZDC–phosphotriester analogs of PtdIns(4,5)P_2, PtdIns(3,4)P_2 and PtdIns(3,4,5)P_3 were recently employed to demonstrate a specific PtdIns(3,4,5)P_3–αCOP interaction in Golgi coatomer [45].

In the current study, we have photoaffinity-labeled human profilin I with three PtdIns(4,5)P_2 photoaffinity probes, each of which samples a different bilayer environment (Figure 1). The [^{3}H]BZDC–Ins(1,4,5)P_3 probe is a PtdIns(4,5)P_2 mimic, as the P-1-(*O*-3-BZDC–aminopropyl) phosphodiester resembles a *2-desacyl* phosphoinositide 4,5-*bis*phosphate analog [33]. The [^{3}H]BZDC–*acyl*-PtdIns(4,5)P_2 probe has the benzophenone photophore incorporated at the hydrophobic bilayer region of the *sn*-1 acyl chain, whereas the [^{3}H]BZDC–*triester*-PtdIns(4,5)P_2 probe has its photoreactive group linked at P-1, allowing access to the interface between the polar head group and the hydrophobic lipid chains.

The covalent photolabeling of human profilin with the [^{3}H]BZDC–Ins(1,4,5)P_3 probe could be displaced using PtdIns(4,5)P_2 or adenophostin A as competing ligands,

suggesting that the 4,5-*bis*phosphate moiety and a sufficiently hydrophobic phosphodiester (or equivalent) linked moiety are both important recognition elements. Failure of a large excess of the PtdIns(4,5)P_2 head group, Ins(1,4,5)P_3, to displace labeling by the photoprobes is consistent with the report that human profilin does not bind Ins(1,4,5)P_3 [46]. Displacement of photolabeling by [^{3}H]BZDC–Ins(1,4,5)P_3 and PtdIns(4,5)P_2 probes by the Ins(1,4,5)P_3 hyperagonist adenophostin A [34] (see Figures 1 and 2) is consistent with the presence of correctly oriented 4,5-*bis*phosphate and lipophilic moieties, and suggests that the drug may have novel effects on cytoskeletal remodeling. The *acyl*-PtdIns(4,5)P_2 probe predominantly showed labeling of phospholipid micelles by self-cross-linking. Indeed, addition of PtdIns(4,5)P_2 merely enhanced the intensity of the fast-moving cross-linked micelles that migrate at the dye front. A fourfold longer exposure of the gel to X-ray film (as shown in Figure 2c) showed that profilin was indeed covalently modified, however, albeit with lower efficiency than with the other two probes. Labeling by the triester probe was also of relatively low efficiency, suggesting that with the *bis*phosphate and diacylglyceryl pockets appropriately occupied, positioning of the BZDC group was inappropriate for effective protein modification. Thus, the PtdIns(4,5)P_2 mimic, [^{3}H]BZDC–Ins(1,4,5)P_3, proved to be the optimal ligand to map the PtdIns(4,5)P_2-binding site on the protein.

The effect of metal ions on the photoaffinity labeling of profilin is intriguing, and is consistent with previous observations of the effect of divalent cations on profilin function. In physiological Mg^{2+} concentrations, profilin binds to actin monomers, and accelerates nucleotide exchange, but the profilin–ATP–actin complex can add to the barbed end of filaments, and this appears to be followed by coupled profilin release and ATP hydrolysis [47,48]. In millimolar Ca^{2+} concentrations and low Mg^{2+}, profilin acts predominantly as an actin monomer sequestering agent, inhibiting addition of bound actin to the barbed end. Formation of higher oligomers of profilin has been reported previously [49]. We suspect that the effects observed may reflect a metal-ion-induced distortion or aggregation in the lipid structure [50–52]. Presumably the effects of Ca^{2+} reflect a change in the conformation that disfavors the photophore–protein contact, whereas Ba^{2+} appeared to enhance the tethered photophore–protein interaction. The apparent higher-order multimers observed in the Ba^{2+} labeling was puzzling, but suggested that the head group may interact with one profilin, whereas the photoreactive tail might react with another molecule.

Binding-site mapping of the protein yielded a peptide with the radiolabel on the fourth residue (alanine) of the recombinant protein (Figure 3). In biological systems, the most effective H-atom donors for the benzophenone diradical include backbone C–H bonds in amino acids, polypeptides, and carbohydrates. Particularly reactive sites include the electron-rich tertiary centers such as C_γ–H of leucine, and C_β–H of valine, and CH_2 groups adjacent to heteroatoms in lysine, arginine and methionine [40]. It is the site of hydrophobic or aromatic interactions between the benzophenone moiety and the protein, as well as the anchoring effect of the inositol polyphosphate head group, however, that ultimately determine which residue has the correct proximity for efficient covalent modification. The average distance of the benzophenone moiety from the charged 4,5-*bis*phosphates on the inositol ring has been calculated to be 7–8 Å (M. Ceruso and A.C., unpublished observations).

On the basis of comparison with regions of gelsolin known to confer binding to PtdIns(4,5)P_2 and by direct analysis, the carboxy-terminal 11 residues of human profilin I (residues 126–136) have been implicated in the recognition of the *bis*phosphate head group of PtdIns(4,5)P_2 [25]. Other studies had also shown that fluorescence quenching of Trp3 and Trp31 occurred in profilin upon binding to PtdIns(4,5)P_2 [27]. Interestingly, the amino- and carboxy-terminal regions of profilin form antiparallel α-helical structures in the crystalline state in the absence of phospholipids. This region presents a largely hydrophobic face with distinctive regions of positive charge that also participates in actin binding. A recent report [13] indicates that PtdIns(4,5)P_2 competes effectively for binding of profilin I to poly-(L-proline), as this isoform and not profilin II can be eluted from a poly-(L-proline) column using PtdIns(4,5)P_2. Thus, the observations reported herein are consistent with models in which the acyl chains of the diacylglyceryl moiety interact with these paired α helices. Other evidence, however, has indicated that residues 69–125 form the PtdIns(4,5)P_2-binding site, with directed mutagenesis supporting a key role for Arg88 [28]. Finally, the large changes in α-helical content occurring in response to binding of the dipalmitoyl derivatives of PtdIns(4,5)P_2 or PtdIns(3,4)P_2 [21] suggest that complex conformational shifts may occur as a result of the ligand–protein complexation. To date, however, no effort has been made to determine how the substitution of a saturated acyl chain for a polyunsaturated acyl chain at the glyceryl *sn*-2 position affects profilin–phosphoinositide binding. A difference is likely, as activation of protein kinase B is several times higher with the natural PtdIns(3,4,5)P_3 than with a dipalmitoyl analog [53].

A computer model was developed to determine whether the calculated molecular geometry of a putative complex between profilin I and the photoactivatable analog of PtdIns(4,5)P_2 was consistent with the observed modification of Ala4 of the recombinant protein. Thus, an energy-minimized model of profilin I with BZDC–Ins(1,4,5)P_3

was calculated (Figure 4) using the average solution structure of human profilin I [3]. The structure was then equilibrated with the ligand, after the carbonyl oxygen of the benzophenone was fixed at a distance of 3.0 Å from the C_α–H on Ala4 (Ala1 of native profilin I). Figure 4 suggests a model to rationalize the binding observed with the BZDC–Ins(1,4,5)P_3 probe. Thus, if the 4,5-*bis*phosphate groups on the inositol ring are allowed to interact with Arg135 and Arg136 of the carboxy-terminal helix, the aminopropyl-linked benzophenone then becomes proximal to the amino-terminal helix.

The studies reported herein demonstrate that Ala1 of human profilin I is located within 3.1 Å of the carbonyl oxygen of the benzophenone photophore [40]. This site of the [^{3}H]BZDC–aminopropyl-linked photoprobe would approximately correspond to the C–4 carbon of a normal acyl chain, as the aminopropyl linker mimics the three-carbon glycerol linker in PtdIns(4,5)P_2. The modeling of this photoreactive probe into the three-dimensional structure of profilin I shows that this PtdIns(4,5)P_2-mimicking ligand nestles between the amino-terminal hydrophobic helix and carboxy-terminal basic region.

Significance

Profilin is a small actin-binding protein, ubiquitous and necessary for normal cell growth and function in eukaryotic organisms. Although the interactions of profilin with its three known ligands (actin monomers, phosphatidylinositol 4,5-*bis*phosphate (PtdIns(4,5)P_2) and poly-(L-proline)) have been well characterized *in vitro*, how these properties affect cellular physiology remains unresolved. By binding to PtdIns(4,5)P_2, profilin is able to inhibit its hydrolysis by phospholipase C-γ_1. The precise site of interaction of the protein with PtdIns(4,5)P_2 is of great interest to numerous researchers in biochemistry and cell biology.

Three photoaffinity analogs of PtdIns(4,5)P_2 were used to sample the different bilayer environments. These probes showed specificity in their affinity for human profilin I, with the ligands PtdIns(4,5)P_2 and adenophostin A showing displacement of the photoaffinity labeling. The labeling was not displaced by excess Ins(1,4,5)P_3, demonstrating that the protein must interact with both the acyl chains and the 4,5-*bis*phosphate at the binding interface. We used one of these specific probes, [^{3}H]4-benzoyldihydrocinnamoyl (BZDC)–Ins(1,4,5)P_3, to map the PtdIns(4,5)P_2-binding site of the protein. Sequencing of a radiolabeled peptide fragment revealed that the benzophenone had covalently modified Ala4 near the amino terminus of the recombinant profilin I. This result, in conjunction with molecular modeling, strongly supports the hypothesis that the PtdIns(4,5)P_2-binding site resides in the hydrophobic, conserved pocket created by the amino- and carboxy-terminal helices.

Materials and methods

Chemicals

P-1-(*O*-3-aminopropyl)-D-*myo*-Ins(1,4,5)P_3 was synthesized from methyl α-D-glucopyranoside as previously described [30]. The corresponding [^{3}H]BZDC–Ins(1,4,5)P_3 probe was prepared by coupling the P-1-(*O*-3-aminopropyl)-D-*myo*-Ins(1,4,5)P_3 with the [^{3}H]BZDC–NHS ester [54]. The synthesis of the [^{3}H]BZDC–*acyl* PtdIns(4,5)P_2 probe was achieved from chiral intermediates synthesized from methyl-D-glucopyranoside and 1,2-isopropylidene-*sn*-glycerol, followed by modification to contain the benzophenone photophore [31]. The [^{3}H]BZDC–*triester*-PtdIns(4,5)P_2 probes were also prepared as previously described [32]. All [^{3}H]BZDC–labeled probes were used in their triethylammonium salt forms. Specific activities of all the BZDC derivatives were 35-42.5 Ci/mmol, depending on the batch of [^{3}H]BZDC–NHS ester used. D-*myo*-Ins(1,4,5)P_3 and PtdIns(4,5)P_2 were synthesized as described [30,31] and used in their sodium salt forms. Adenophostin A was obtained from Sankyo Company (Japan). All other reagents were obtained from Sigma Chemical Co. (St. Louis, MO). Solutions were made in Nanopure® (ultrafiltered, distilled and deionized) water.

Photoaffinity labeling with the [^{3}H]BZDC probes

Profilin I was expressed in the vector pMW172 and purified on a poly(L-proline) affinity column as previously described [11]. An aliquot of profilin I (1 μg) was incubated with 0.2-0.4 μCi (0.1 μM) of the [^{3}H]BZDC probe (specific activity, 42.5 Ci/mmol) in buffer A (10 mM Tris pH 7.5). A 1,000-fold excess (0.1 mM) of the competitor (Ins(1,4,5)P_3, PtdIns(4,5)P_2, or adenophostin A) was used to determine the affinity and specificity of binding. The solution was incubated on ice for 10 min and then photolyzed at 360 nm (1900 μW/cm^2) for 45 min in a 96-well plate. Proteins were separated by electrophoresis (SDS-18% polyacrylamide gel electrophoresis PAGE), the gel Coomassie Blue stained and then destained with 45% methanol–10% acetic acid. The gel was then impregnated with En^{3}Hance (NEN Life Science Products, Boston, MA) solution for 1 h according to the manufacturer's instructions, and 50% polyethylene glycol (PEG 1450) was used to shrink the Laemmli gel back to original size [55]. The gel was then dried and autoradiography performed (15 days exposure at −80°C, XAR-5 X-ray film). No covalent incorporation of the photoprobe occurred in the absence of irradiation. All photolabeling experiments were repeated in three independent replicates.

Binding-site mapping

Large-scale photolabeling of profilin was conducted to obtain covalently modified peptides for sequencing. Thus, 500 μg (35 nmol) of profilin I, 5 μCi [^{3}H]BZDC–Ins(1,4,5)P_3 (specific activity, 42.5 Ci/mmol), and unlabeled BZDC–Ins(1,4,5)P_3 (final concentration, 70 μM) were diluted with buffer A to a final volume of 500 μl. Photolabeling was performed in 10 mM Tris–HCl buffer (pH 7.5) as described above. Protein was precipitated with trichloroacetic acid, and the pellet was washed with cold acetone and then dried *in vacuo*. The sample was dissolved in 100 μl of 70% formic acid, a 500-fold excess of CNBr added, and the digestion performed under argon, in darkness, for 24 h at room temperature [39]. The sample was then diluted tenfold with water and lyophilized. An analogous procedure was performed with unmodified recombinant profilin I.

Samples of CNBr digests of the photoaffinity-labeled and the unmodified protein were analyzed by MALDI–TOF MS using a Bruker ProteinTOF® operating in positive ion reflectron mode. Two different desorption matrices, α-cyano-4-hydroxycinnamic acid and sinapinic acid were used (Aldrich Chemical Co., Milwaukee, WI). A 50 mM stock solution of the matrix was made by dissolving it in 30% acetonitrile (v/v). The water used to make the solution contained 0.1% TFA to assist in dissolving the proteins. This stock solution was stored in darkness, and is stable for only a few days. The matrix stock solution (5 μl) was placed in a conical 1.5 ml polypropylene tube and 0.5 μl of the modified and unmodified protein solutions (9 μM) to be analyzed were added. The solution was briefly mixed by vortexing. A small aliquot

(< 0.5 µl) of the matrix–protein mixture was then applied to the flat metal probe and dried at room temperature. The probe was then inserted through a vacuum lock into the MS.

From a separate CNBr digest of [^{3}H]-BZDC–Ins(1,4,5)P_3-labeled profilin I, peptide fragments were dissolved in 200 µl guanidinium hydrochloride (6 M, 50 mM Tris, pH 8.0), and then separated by HPLC using a C_{18} reversed phase column (4.6 mm × 25 cm, Zorbax 300 SB-C-18), by elution at 0.5 ml/min with a linear gradient from 0 to 80% acetonitrile, with 0.06% TFA in both mobile phase components. Eluted peptides were monitored at an absorbance of 210 nm, and collected automatically. Radiolabeled fractions were determined by LSC, and the radioactive fractions lyophilized to near dryness and sequenced by standard Edman degradation chemistry using an ABI 477 protein sequencer. The amino acid phenylthiohydantoin derivative reactions were then collected manually and radioactivity was measured by LSC.

Molecular modeling

The average structure of human profilin I [3] was downloaded into INSIGHT II (Biosym Technologies, version 2.3.0) from the Brookhaven Database (identification code 1PFL). The acidic and basic residues were assigned a charge of +1 and −1, respectively. A charge of 0.5 was assigned to the histidine residues. A model of aminopropyl-tethered BZDC–Ins(1,4,5)P_3 was constructed in the builder module and energy minimized. The benzophenone carbonyl oxygen was then locked at a distance of 3.0 Å from the C_α–H on Ala1 of profilin I. We assigned the AMBER forcefield to this model. This model was used for molecular dynamics simulations (Discover, Biosym 1994) in vacuum to investigate the possible dynamic behavior of the conformation of the ligand. The structure was equilibrated by performing dynamics at 300 K during 10 ps.

Acknowledgements

We thank J.T. Elliott (University at Stony Brook, USB, Stony Brook, NY) for advice and M.R. Ziebell (USB and The University of Utah, UU, Salt Lake City, UT), B. Mehrotra (USB and UU), S. Reddy (USB), S. Mitchell (UU), M. B. Yaffe (Harvard Medical School, HMS, Boston, MA), and B. C. Duckworth (HMS) for assistance with molecular modeling. The [^{3}H]BZDC–NHS ester reagent was generously provided by D. G. Ahern (NEN Life Science Products, Boston, MA). We are grateful to P.A. Janmey and L.A. Flanagan (Brigham and Women's Hospital, Boston, MA) for critical review of the manuscript. The adenophostin A was a generous gift of the Sankyo Company, Japan. Edman degradation analysis was performed at UU by R. Schackmann, and MALDI-TOF analysis was performed at USB by Q.-M. Gu using a Bruker ProteinTOF® acquired with funding from the National Science Foundation, the USB campus, and the USB Center for Biotechnology/New York Science and Technology Foundation.

Financial support was provided by the National Institutes of Health (Grants NS 29632 to G.D.P. and GM 53236 to D.J.K.) and in part by NEN Life Science Products.

References

1. Sohn, R.H. & Goldschmidt-Clermont, P.J. (1994). Profilin: at the crossroads of signal transduction and the actin cytoskeleton. *Bioessays* **16**, 465-472.
2. Theriot, J.A. & Mitchison, T.J. (1993). The three faces of profilin. *Cell* **75**, 835-838.
3. Metzler, W.J., Framer, B.T.N., Constantine, K.L., Friedrichs, M.S., Lavoie, T. & Mueller, L. (1995). Refined solution structure of human profilin I. *Protein Sci.* **4**, 450-459.
4. Goldschimdt-Clermont, P.J., Machesky, L.M., Baldassare, J.J. & Pollard, T.D. (1990). The actin binding protein profilin binds to PIP_2 and inhibits its hydrolysis by phospholipase C. *Science* **247**, 1575-1578.
5. Hartwig, J., Chambers, K., Hopcia, K. & Kwiatkowski, D. (1989). Association of profilin with filament-free regions of human leukocyte and platelet membranes and reversible membrane-binding during platelet activation. *J. Cell Biol.* **109**, 1571-1579.
6. Ostrander, D.B., Gorman, J.A. & Carman, G.M. (1995). Regulation of profilin localization in *Saccharomyces cerevisiae* by phosphoinositide metabolism. *J. Biol. Chem.* **270**, 27045-27050.
7. Singh, S.S., Chauhan, A., Murakami, N. & Chauhan, V.P. (1996). Profilin and gelsolin stimulate phosphatidylinositol 3-kinase activity. *Biochemistry* **35**, 16544-16549.
8. Kaiser, D.A. & Pollard, T.D. (1996). Characterization of actin and poly-L-proline binding sites of *Acanthamoeba* profilin with monoclonal antibodies and by mutagenesis. *J. Mol. Biol.* **256**, 89-107.
9. Metzler, W.J., Bell, A.J., Ernst, E., Lavoie, T.B. & Mueller, L. (1994). Identification of the poly-L-proline binding site on human profilin. *J. Biol. Chem.* **269**, 4620-4625.
10. Reinhard, M., Giehl, K., Abel, K., Haffner, C., Jarchau, T., Hoppe, V., Jockusch, B.M. & Walter, U. (1995). The proline-rich focal adhesion and microfilament protein VASP is a ligand for profilins. *EMBO J.* **14**, 1583-1589.
11. Gieselmann, R., Kwiatkowski, D.J., Janmey, P.A. & Witke, W. (1995). Distinct biochemical characteristics of the two human profilin isoforms. *Eur. J. Biochem.* **229**, 621-628.
12. Lambrechts, A., Van Damme, J., Goethals, M., Vanderkerchove, J. & Ampe, C. (1995). Purification and characterization of bovine profilin II: actin, poly-(L-proline) and inositol phospholipid binding. *Eur. J. Biochem.* **230**, 281-286.
13. Lambrechts, A., Verschelde, J.L., Jonckheere, V., Goethals, M., Vandekerckhove, J. & Ampe, C. (1997). The mammalian isoforms display complementary affinities for PIP_2 and proline rich sequences. *EMBO J.* **16**, 484-494.
14. Thorn, K.S., Christensen, H.E.M., Shigeta, R., Huddler, D., Shalaby, L., Lindberg, U., Chua, N.-H. & Schutt, C.E. (1997). The crystal structure of a major allergen from plants. *Structure* **5**, 19-32.
15. Haugwitz, M., Noegel, A., Karakesisoglou, J. & Schleicher, M. (1994). *Dictyostelium amoebae* that lack G-actin-sequestering profilins show defects F-actin content, cytokinesis and development. *Cell* **79**, 303-314.
16. Balasubramanian, M., Hirani, B., Burke, J. & Gould, K. (1994). The *Schizosaccharomyces pombe* cdc3+ gene encodes a profilin essential for cytokinesis. *J. Cell Biol.* **125**, 1289-1301.
17. Magdolen, V., Ochsner, U., Muller, G. & Bandlow, W. (1988). The intron-containing gene for yeast profilin (PFY) encodes a vital function. *Mol. Cell Biol.* **8**, 5108-5120.
18. Verheyen, E. & Cooley, L. (1994). Profilin mutations disrupt multiple actin-dependent processes during *Drosophila* development. *Development* **120**, 717-728.
19. Cooley, L., Verheyen, E. & Ayers, K. (1992). *chickadee* encodes a profilin required for intercellular cytoplasm transport during *Drosophila* oogenesis. *Cell* **69**, 173-184.
20. Carlier, M. & Pantaloni, D. (1997). Control of actin dynamics in cell motility. *J. Mol. Biol.* **269**, 459-567.
21. Machesky, L., Reeves, E. & Wientjes, F. (1997). Mammalian actin-related protein 2/3 complex localizes to regions of lamellipodial protrusion and is composed of evolutionarily conserved proteins. *Biochem. J.* **328**, 105-112.
22. Schluter, K., Jockusch, B. & Rothkegel, M. (1997). Profilins as regulators of actin dynamics. *Biochim. Biophys. Acta* **1359**, 97-109.
23. Witke, W., Sharpe, A. & Kwiatkowski, D. (1993). Profilin deficient mice are not viable. *Mol. Biol. Cell* **4**, 149a.
24. Schutt, C.E., Myslik, J.C., Rozycki, M.D., Goonesekere, N.C.W. & Lindberg, U. (1993). The structure of crystalline profilin-actin. *Nature* **365**, 810-816.
25. Yu, F.-X., Sun, H.-Q., Janmey, P.A. & Yin, H.L. (1992). Identification of a polyphosphoinositide binding sequence in an actin monomer-binding domain of gelsolin. *J. Biol. Chem.* **267**, 14616-14621.
26. Fedorov, A.A., Magnus, K.A., Graupe, M.H., Lattman, E.E., Pollard, T.D. & Almo, S.C. (1994). X-ray structures of isoforms of the actin-binding protein profilin that differ in their affinity for phosphatidylinositol phosphates. *Proc. Natl Acad. Sci. USA* **91**, 8636-8640.
27. Raghunathan, V., Mowery, P., Rozycki, M., Lindberg, U. & Schutt, C. (1992). Structural changes in prolifin accompany its binding to phosphatidylinositol 4,5 bisphosphate. *FEBS Lett.* **297**, 46-50.
28. Sohn, R.H., Chen, J., Koblan, K.S., Bray, P.F. & Goldschmidt-Clermont, P.J. (1995). Localization of a binding site for phosphatidylinositol 4,5-bisphosphate on human profilin. *J. Biol. Chem.* **270**, 21114-21120.
29. Lu, P.J., Shieh, W.R., Rhee, S.G., Yin, H.L. & Chen, C.S. (1996). Lipid products of phosphoinositide 3-kinase bind human profilin with high affinity. *Biochemistry* **35**, 14027-14034.
30. Dormán, G., Chen, J. & Prestwich, G.D. (1995). Synthesis of D-*myo*-P-1-(O-aminopropyl)-inositol-1,4,5-trisphosphate affinity probes from α-D-glucose. *Tetrahedron Lett.* **36**, 8719-8722.
31. Chen, J., Profit, A.A. & Prestwich, G.D. (1996). Synthesis of photoactivatable 1,2-*O*-diacyl-*sn*-glycerol derivatives of 1-L-phosphatidyl-D-*myo*-inositol 4,5-bisphosphate (PtdInsP_2) and 3,4,5-trisphosphate (PtdInsP_3) *J. Org. Chem.* **61**, 6305-6312.
32. Gu, Q.-M. & Prestwich, G.D. (1996). Synthesis of phosphotriester analogues of the phosphoinositides PtdIns(4,5)P_2 and PtdIns(3,4,5)P_3. *J. Org. Chem.* **61**, 8642-8647.

33. Prestwich, G.D. (1996). Touching all the bases: synthesis of inositol polyphosphate and phosphoinositide affinity probes from glucose. *Accounts Chem. Res.* **29**, 503-513.
34. Takahashi, M., Tanazawa, K. & Takahashi, S. (1994). Adenophsotins, newly discovered metabolites of *Penicillium brevicompactum*, act as potent agonists of the inositol 1,4,5-trisphosphate receptor. *J. Biol. Chem.* **269**, 369-372.
35. Chaudhary, A. & Prestwich, G.D. (1994). Adenophostins: newly discovered metabolites of *Penicillium brevicompactum* as potent agonists of the Ins(1,4,5)P_3 receptor. *Chemtracts-Org. Chem.* **7**, 111-114.
36. Mourey, R.J., Estevez, V.A., Marecek, J.F., Barrow, R.K., Prestwich, G.D. & Snyder, S.H. (1993). Inositol 1,4,5-trisphosphate receptors: mapping the inositol 1,4,5-trisphosphate binding site with photoaffinity ligands. *Biochemistry* ***32***, 1719-1726.
37. Hirata, M., Kanematsu, T., Sakuma, K., Koga, T., Watanabe, Y., Ozaki, S. & Yagisawa, H. (1994). D-*myo*-Inositol 1,4,5-trisphosphate binding domain of phospholipase C-δ1. *Biochem. Biophys. Res. Commun.* **205**, 1563-1571.
38. Tall, E., Dormán, G., Garcia, P., Chen, J., Profit, A.A., Shah, S., Gu, Q.-M., Chaudhary, A., Prestwich, G.D. & Rebecchi, M.J. (1997). Phosphoinositide-binding specificity among phospholipase C isozymes as determined by photocrosslinking to novel substrate and product analogs. *Biochemistry* **36**, 7239-7248.
39. Charbonneau, H. (1989). Strategies for obtaining partial amino acid sequence data from small quantities (< 5 nmol) of pure or partially purified protein. In *A Practical Guide to Protein and Peptide Purification for Microsequencing*; 2nd edn. (Matsudaira, P.T., ed.), pp 131, Academic Press Inc., San Diego, CA.
40. Dormán, G. & Prestwich, G.D. (1994). Benzophenone photophores in biochemistry. *Biochemistry* **33**, 5661-5673.
41. Prestwich, G.D., Dormán, G., Elliott, J.T., Marecak, D.M. & Chaudhary, A. (1997). Benzophenone photophores for phosphoinositides, peptides, and drugs. *Photochem. Photobiol.* **65**, 222-234.
42. Theibert, A.B., Estevez, V.A., Mourey, R.J., Marecek, J.F., Barrow, R.K., Prestwich, G.D. & Snyder, S.H. (1992). Photoaffinity labeling and characterization of isolated inositol 1,3,4,5-tetrakisphosphate and inositol hexakisphosphate-binding proteins. *J. Biol. Chem.* **267**, 9071-9079.
43. Mehrotra, B., Elliott, J.T., Chen, J., Olszewski, J.D., Profit, A.A., Chaudhary, A., Fukuda, M., Mikoshiba, K. & Prestwich, G.D. (1997). Selective photoaffinity labeling of the inositol polyphosphate binding C2B domains of synaptotagmins. *J. Biol. Chem.* **272**, 4237-4244.
44. Hammonds-Odie, L.P., Jackson, T.R., Profit, A.A., Blader, I.J., Turck, C.W., Prestwich, G.D. & Theibert, A.B. (1996). Identification and cloning of centaurin-α - a novel phosphatidylinositol 3,4,5-trisphosphate-binding protein from rat brain. *J. Biol. Chem.* **271**, 18859-18868.
45. Chaudhary, A., Gu, Q.-M., Thum, O., Profit, A.A., Qi, Y., Jeyakumar, L., Fleischer, S. & Prestwich, G.D. (1998). Specific interaction of Golgi coatomer protein αCOP with phosphatidylinositol 3,4,5-trisphosphate. *J. Biol. Chem.* **273**, 8344-8350.
46. Machesky, L.M., Goldschmidt-Clermont, P.J. & Pollard, T.D. (1990). The affinities of human platelet and *Acanthamoeba* profilin isoforms for polyphosphoinositides account for their relative abilities to inhibit phospholipase C. *Cell. Regul.* **1**, 937-950.
47. Perelroizen, I., Didry, D., Christensen, H., Chua, N.H. & Carlier, M.F. (1996). Role of nucleotide exchange and hydrolysis in the function of profilin in actin assembly. *J. Biol. Chem.* **271**, 12302-12309.
48. Perelroizen, I., Carlier, M.F. & Pantaloni, D. (1995). Binding of divalent cation and nucleotide to G-actin in the presence of profilin. *J. Biol. Chem.* **270**, 1501-1508.
49. Babich, M., Foti, L.P.R., Sykaluk, L.L. & Clark, C.R. (1996). Profilin binds tetramers that bind to G-actin. *Biochem. Biophy. Res. Commun.* **218**, 125-131.
50. Hendrickson, H. & Fullington, J. (1965). Stabilities of metal complexes of phospholipids: Ca(II), Mg(II), and Ni(II) complexes of phosphatidylserine and triphosphoinositide. *Biochemistry* **4**, 1599-1605.
51. Hirai, M., Takizaka, T., Yabuki, S., Nakata, Y., Hirai, T. & Hayashi, K. (1996). Salt-dependent phase behaviour of the phosphatidylinositol 4,5-bisphosphate-water system. *J. Chem. Soc. Faraday Trans.* **92**, 1493-1498.
52. Flanagan, L.A., Cunningham, C.C., Chen, J., Prestwich, G.D., Kosik, K.S. & Janmey, P.A. (1997). The structure of divalent cation-induced aggregates of PIP_2 and their alteration by gelsolin and tau. *Biophys. J.* **73**, 1440-1447.
53. Stokoe, D., Stephens, L.R., Copeland, T., Gaffney, P.R., Reese, C.B., Painter, G.F., Holmes, A.B., McCormic, F. & Hawkins, P.T. (1997). Dual role of phosphatidylinositol-3,4,5,-trisphosphate in the activation of protein kinase B. *Science* **277**, 567-570.
54. Olszewski, J.D., Dormán, G., Elliott, J.T., Hong, Y., Ahern, D.G. & Prestwich, G.D. (1995). Tethered benzophenone reagents for the synthesis of photoactivatable ligands. *Bioconj. Chem.* **6**, 395-400.
55. Mohamed, M.A., Lerro, K.A. & Prestwich, G.D. (1989). Polyacrylamide gel miniaturization improves protein visualization and autoradiographic detection. *Anal. Biochem.* **177**, 287-290.

Because *Chemistry & Biology* operates a 'Continuous Publication System' for Research Papers, this paper has been published via the internet before being printed. The paper can be accessed from http://biomednet.com/cbiology/cmb – for further information, see the explanation on the contents pages.